Journal of Organometallic Chemistry 846 (2017) 312–320

Contents lists available at ScienceDirect

Journal of Organometallic Chemistry

journal homepage: www.elsevier.com/locate/jorganchem

Apoptosis in vitro in PC-12 cells induced by an organometallic Ir(III) complex through a ROS-mediated mitochondrial pathway

Xian-Lan Hong [a, *], Yu-Huan Zhou [a], Chuan-Chuan Zeng [b], Xiao-Chao Wu [a], Yun-Jun Liu [b, **]

[a] Department of Chemistry, Shaoguan University, Shaoguan, Guangdong, 512005, PR China
[b] School of Pharmacy, Guangdong Pharmaceutical University, Guangzhou, 510006, PR China

ARTICLE INFO

Article history:
Received 6 June 2017
Received in revised form
2 July 2017
Accepted 5 July 2017
Available online 8 July 2017

Keywords:
Ir(III) complex
Cytotoxicity
ROS
Apoptosis
Cell cycle distribution

ABSTRACT

An Ir(III) organometallic complex, $[Ir(ppy)_2(paip)]PF_6$ (**1**), (ppy and paip denote 2-phenylpyridine and 2-(4-aminophenyl) imidazo [4,5-f] [1,10] phenanthroline, respectively) was synthesized and characterized by elemental analysis, ESI-MS, ^1H and ^{13}C NMR. The cytotoxic activity in vitro of the complex was evaluated by MTT (MTT = (3-(4,5-dimethylthiazol-2-yl)-2,5-diphenyltetrazolium bromide)) method. The complex shows higher cytotoxic activity against PC-12 cells than cisplatin. The intracellular ROS generation and mitochondrial membrane potential (MMP) changes were determined by fluorescent microscope and flow cytometry. The cellular uptake and location of complex **1**, as well as cell cycle distribution and matrigel invasion in PC-12 cells treated with the complex were investigated. Meanwhile, Bcl-2 family proteins expression was also explored by western blot. The results indicate that the complex shows efficient cellular uptake and cumulates in nucleus as well as in mitochondria, and inhibits both the growth at G0/G1 phase and the invasion in extracellular matrix. It is rationally concluded that complex **1** induces apoptosis in PC-12 cell through a ROS-mediated mitochondrial dysfunction pathway with an increase in ROS level and a decrease in MMP.

1. Introduction

The side effect and resistance of platinum-based anticancer drugs have stimulated the research efforts to explore other metal complexes as alternatives to platinum anticancer agents [1–8]. Much attention has been focused on the complexes with a metal center of d^6 electron configuration featuring inert coordination substitution. More and more Ru(II) octahedral polypyridyl complexes were found to have superior antitumor activity and can circumvent the shortcomings of cisplatin to some extent [9–12]. It is well conceivable that the distinctiveness in antitumor behaviors and biological features including toxicity and drug delivery between these Ru(II) complexes and cisplatin analogues mainly stem from the difference of DNA-binding mode; the former interacts with DNA by intercalation between base pairs, and the latter by covalent crosses links resting upon ligand institution reaction [4,13,14]. Recently, Ir(III) complexes have attracted significant interests in developing non-platinum anticancer drugs based on the consideration that the coordination substitution inertness of octahedral low-spin d^6 Ir(III) complexes are more prominent than that of Ru(II) complexes; the mean lifetime for exchange of an aqua ligand of $[Ir(H_2O)_6]^{3+}$ is about 8 orders of magnitude larger than that of $[Ru(H_2O)_6]^{2+}$ [15], and a series of polypyridyl Ir(III) complexes have been synthesized and proved to possess high bioactivity over the last decade [16–21]. On the other hand, the Ru(II) complexes containing a coordinated cation with single charge, such as $[Ru(bpy)(phpy)(dppz)]^+$ [22], $[(\eta^6\text{-}C_6Me_6)Ru(Cl)(pp)]^+$ [23], $[Ru(dtzp)(dppz)Cl]^+$ [24], exhibit better liposolubility, much greater cellular uptake efficiency and better anti-cancer activity than their corresponding complexes with doubly charged cations (namely, $[Ru(bpy)_2(dppz)]^{2+}$, $[(\eta^6\text{-}C_6Me_6)Ru((NH_2)_2CS)(pp)]^{2+}$, $[Ru(dtzp)(dppz)CH_3CN]^{2+}$). The combination of the ease of synthesis and the excellent photophysical and biochemical properties make the biscylometalated Ir(III) complexes with a style of $[Ir(C,N)_2(N,N,N)]^+$ more suitable to be developed as non-platinum anticancer drugs [5,21,25–27]. Meanwhile, it is interesting to find that the ruthenium (II) complexes with the ligand paip were proved

* Corresponding author.
** Corresponding author.
E-mail addresses: hongxianlan@163.com (X.-L. Hong), lyjche@gdpu.edu.cn (Y.-J. Liu).

http://dx.doi.org/10.1016/j.jorganchem.2017.07.004
0022-328X/

to show superior in vitro anticancer activity [28,29]. In order to obtain more anticancer information of Ir(III) complexes, herein, an organometallic paip-containing complex (**1**) was synthesized (Scheme 1). The cytotoxicity in vitro against several cancer cell lines and the action mechanism of the complex were investigated in detail using cytological experimental methods.

2. Materials and methods

Cancer cell lines of SGC-7901 (human gastric adenocarcinoma), SiHa (human cervical carcinoma), A549 (human lung carcinoma), BEL-7402 (human hepatocellular carcinoma), PC-12 (pheochromocytoma), HeLa (human cervical cancer), HepG2 (human hepatocellular carcinoma), normal NIH3T3 (mouse embryonic fibroblast) cells, were purchased from the American Type Culture Collection. $IrCl_3 \cdot 3H_2O$, ppy (2-phenylpyridine), and all the other reagents and solvents were commercially obtained and used without further purification, double-distilled water with Ultrapure MilliQ was used in all experiments. RPMI 1640 was purchased from Sigma.

Elemental analysis (CHN) was performed with a Perkin-Elmer 240Q elemental analyzer. Electrospray ionization mass spectrum (ESI–MS) was carried out on a LCQ system (Finnigan MAT, USA) using acetonitrile as mobile phase. NMR spectra (^1H and ^{13}C) were conducted on a Varian 500 MHz spectrometer with DMSO-d_6 as solvent and TMS as an internal standard at ambient temperature.

2.1. The synthesis of $[Ir(ppy)_2(paip)]PF_6$ (**1**)

A mixture of *cis*-$[Ir(ppy)_2Cl]_2$ [26,27] (0.16 g, 0.15 mmol), paip [30] (0.083 g, 0.30 mmol) and 21 ml CH_2Cl_2/CH_3OH (2:1, v/v) was refluxed at 50 °C under the protection of argon for 9 h. Upon cooling to ambient temperature, NH_4PF_6 (0.12 g, 0.75 mmol) was added with keeping the stirring for 2 h, then the reaction mixture was evaporated to dryness under reduced pressure. The obtained solid was dissolved in 20 mL CH_2Cl_2, after filtering out the insoluble substance, the filtrate was evaporated with rotary vacuum evaporator. The crude product, an ocher solid, was purified by column chromatography on neutral alumina with dichloromethane/acetone (1:8, v/v) as eluent. The orange band was collected, upon removing off the solvent by using rotary evaporator again, the desired product (orange powder) was obtained. Yied: 0.335 g, 70%. Anal. Calc for $C_{41}H_{29}N_7IrPF_6$: C, 51.46; H, 3.05; N, 10.25%. Found: C, 51.37; H, 3.22; N, 10.36%. IR (KBr, cm^{-1}): 3384, 2972, 1686, 1608, 1583, 1479, 1455, 845, 759, 558. ^1H NMR (DMSO-d_6): δ 9.14 (d, J = 8.2 Hz, 2H), 8.27 (d, J = 8.1 Hz, 2H), 8.10 (s, 2H), 8.06 (s, 2H), 8.02–7.94 (m, 4H), 7.87 (dd, J = 11.3, 4.5 Hz, 2H), 7.50 (d, J = 4.9 Hz, 2H), 7.06 (d, J = 7.7, 1.2 Hz, 2H), 7.04–6.91 (m, 4H), 6.76 (d, J = 8.7 Hz, 2H), 6.32–6.27 (m, 2H), 5.78 (s, 1H), 4.51 (s, 2H). ^{13}C NMR: 168.88, 156.29, 153.21, 152.42, 151.09, 146.01, 140.64, 138.95, 134.21, 133.81, 133.19, 132.23, 130.02, 128.94, 128.71, 127.89, 127.53, 127.04, 125.81, 124.32, 121.94, 118.31, 115.63. ESI-MS: m/z = 814.5 $[M\text{-}PF_6]^+$.

2.2. Cytotoxic activity in vitro

A common MTT assay procedure was followed in literature [31]. Cells were seeded in 96-well culture plates at a density of 8×10^3 cells per well and incubated overnight at 37 °C in 5% CO_2 atmosphere with 95% relative humidity. The complex **1**, predissolved in DMSO, was added to the wells to reach the final concentrations ranging from 1 to 100 μM. After further incubated for 48 h, the wells were added 20 μL MTT PBS solution (5 mg mL^{-1}) and incubated for another 4 h. The formed formazan crystals were dissolved in 100 μL buffer containing 50% DMF and 20% SDS and read the data of optical density at 490 nm in a microplate spectrophotometer. Control well was prepared by the adding 100 μL culture medium. The IC_{50} values were determined by plotting the percentage of cell viability versus concentration on a logarithmic graph and reading off the control, each experiment was performed in triplicate.

2.3. Apoptosis study

Apoptosis assay was performed with AO/EB staining method [32]. PC-12 cells at a density of 2×10^5 were seeded and incubated in RPMI 1640 (Roswell Park Memorial Institute) with 10% of fetal bovine serum (FBS) onto chamber slides at 37 °C in 5% CO_2 for 24 h. Upon removing the medium, solutions of complex **1** at 10.50 and 21.00 μM in medium with 0.05% DMSO were added and incubated for 24 h, then the cells were washed with ice-cold PBS buffer, fixed with formalin (4%, w/v), and counterstained with AO and EB (100 μg/mL). Samples were observed under a fluorescence microscope (Nikon, Yokohama, Japan) with excitation at 350 nm and emission at 460 nm. Annexin V-FITC/PI double staining assay was used to determine the percentage of apoptotic cells, in briefly, cells (1×10^6) with exposure to complex **1** at 6.25 and 12.5 μM were harvested and fixed with 70% ethanol, and stained with PI (50 μg/mL) and annexin (1 mg/mL) in PBS. The fluorescence at 530 and 575 nm was then equivalently measured with excitation at 488 nm using a FACSCalibur flow cytometry system (Becton, Dickinson, Franklin Lakes, NJ, USA). A minimum of 10,000 cells were analyzed for each sample.

2.4. Cell uptake, mitochondrial location assay and reactive oxygen species (ROS) detection

PC-12 cells were seeded and incubated in 24-well culture plates (4×10^4 cells per well) overnight at 37 °C in a 5% CO_2 incubator, then complex **1** was added to reach a final concentration of 12.5 μM and incubated for another 24 h. Washed with PBS three times, the cells were stained with DAPI (0.5 mg/ml) and MitoTracker® Deep Red FM (80 nM) respectively for detecting the cellar uptake and mitochondrial location of complex **1** *via* imaging under a fluorescent microscopy.

For the detection of intracellular ROS generation induced by complex **1**, PC-12 cells were seeded into six-well plates with

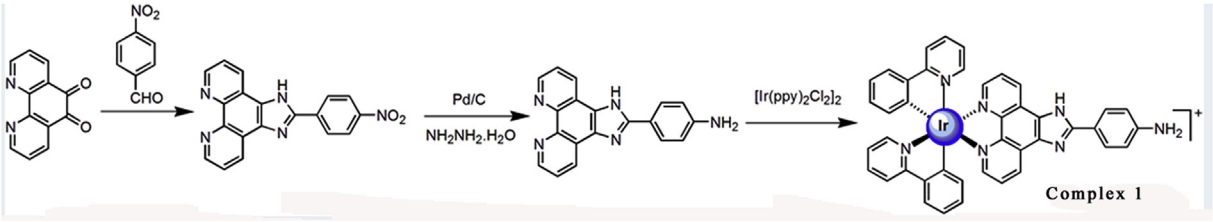

Scheme 1. The synthetic rout of ligand and complex **1**.

2×10^5 cells each well and incubated in RPMI 1640 supplemented with 10% of FBS for 24 h at 37 °C in 5% CO_2. The medium was renewed with medium containing complex **1** (12.5 μM) and incubated for 24 h. After the medium was removed off, the cells were covered with 2′,7′-Dichlorodihydrofluorescein diacetate (H_2DFC-DA) medium solution (10 μM). The treated cells were then washed with cold PBS-EDTA twice, and collected by trypsinization and centrifugation, the resulting cell pellets were resuspended in PBS-EDTA and imaged under a fluorescent microscope. The DCF fluorescent intensity was determined by flow cytometry, the level of intracellular ROS was expressed as the mean fluorescence intensity. Data acquisition and analysis were carried out with BD FACSDiva software v6.0.

2.5. Cell cycle arrest by flow cytometry

Following the treatment with complex **1** (12.5 μM) for 24 h in six-well plates (Costar, Corning Corp, New York, USA), PC-12 cells were trypsinized and incubated with 70% ethanol (v/v) overnight at −20 °C for fixation. The cells were centrifuged (10 min at 1000 r/min) and washed twice with ice-cold PBS. After incubation for 24 h, the cell layer washed with cold PBS and re-suspended, then twenty microliters of RNAse (0.2 mg/mL) and 20 μL of propidium iodide (0.02 mg/mL) were added to the cell suspensions and incubated in the dark at 37 °C for 30 min. The samples were analyzed with a FACSCalibur flow cytometry. The number of cells analyzed for each sample was 10,000, and the acquired data were analyzed with ModFit LT3.2 [33].

2.6. Cell invasion assay

Matrigel chamber assays were conducted to investigate the invasiveness of PC-12 cell according to the manufacturer's instructions. Approximately 4×10^4 cells were added to the upper chamber coated with a ECM (extracellular matrix) membrane with 8.0 μm pores and cultured in serum free RPMI-1640 media and different concentration of complex 1 (6.25 and 12.5 μM), and RPMI 1640 with 20% FBS as chemo-attractant was added to the lower chamber. After incubation for 24 h at 5% CO_2 and 37 °C, non-invading cells were removed from the upper surface with a cotton swab. The invading cells attached on the opposite surface were fixed with 4% paraformaldehyde and stained with 0.1% crystal violet. The cells migrating across the filter were counted and imaged under fluorescent microscopy. Each experiment was repeated at three times to obtain the mean values.

2.7. The expression of caspase and proteins

PC-12 cells were seeded in 3.5 cm dishes in PBS (containing 10% fetal calf serum) with complex **1** at 6.25 and 12.5 μM. After incubation for 24 h, the cells were harvested in lysis buffer, sonicated, and then centrifuged for 25 min at 10,000 g. The supernatant was collected, the concentration of protein in it was determined by BCA assay. SDS-PAGE was performed by loading equal amounts of proteins per lane. Gels were then transferred to poly (vinylidene difluoride) membranes (Millipore) and blocked with 5% nonfat milk in TTBS (Tris-Tween20 buffer saline) buffer for 1 h. Then, the

Table 1
IC_{50} values of the compounds (Comp) against the selected cell lines.

Comp	SGC-7901	SiHa	A549	Bel-7402	PC-12	HeLa	HepG-2
paip	27.3 ± 1.6	40.7 ± 4.2	27.7 ± 1.8	59.8 ± 4.5	>200	25.4 ± 2.2	37.8 ± 2.8
1	46.2 ± 3.8	15.9 ± 1.2	90.2 ± 5.5	24.5 ± 1.3	10.2 ± 1.0	>100	>100
Cisplatin	3.4 ± 0.4	13.3 ± 2.0	13.6 ± 1.1	11.6 ± 1.2	11.4 ± 0.5	6.8 ± 1.1	20.3 ± 1.2

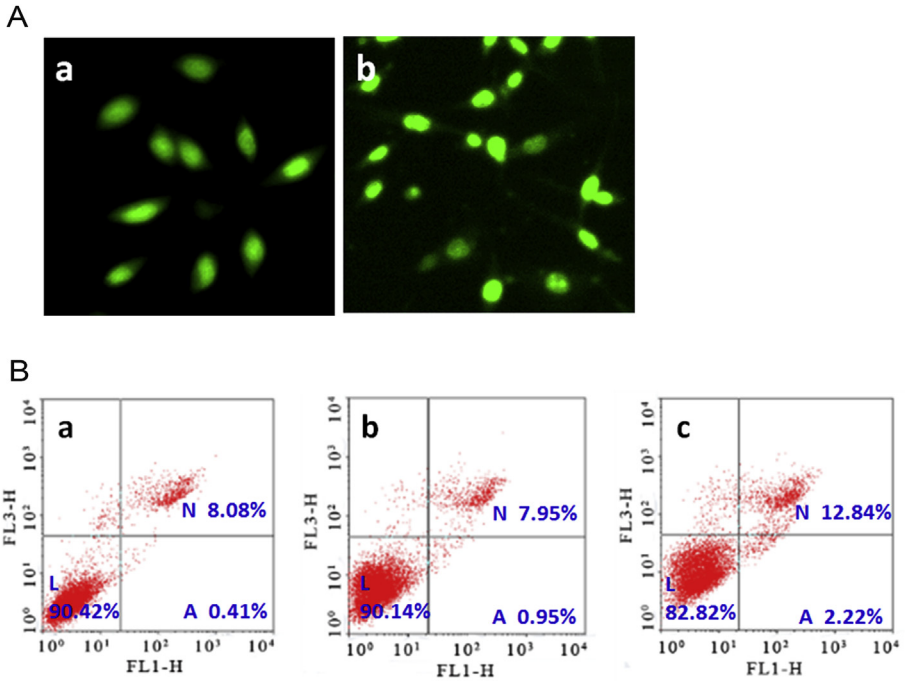

Fig. 1. A Apoptosis in PC-12 cells (a) exposure to 12.5 μM of complex **1** (b) for 24 h and the cells were stained with AO/EB. B The percentage of living (L), necrotic (N), and apoptotic (A) cells was assayed by flow cytometry after PC-12 cell (a) was treated with 6.25 (b) and 12.5 μM of **1** for 24 h and the cells were stained with Annexin V-FITC/PI.

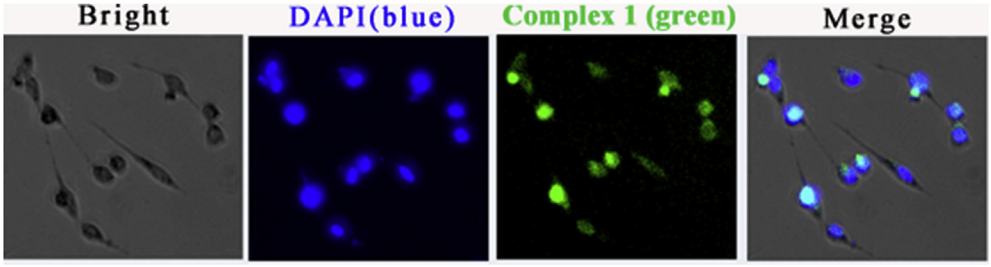

Fig. 2. Images of PC-12 cell exposure to 6.25 μM complex **1** and stained with DAPI.

membranes were incubated with primary antibodies at 1:5000 dilution in 5% nonfat milk overnight at 4 °C and washed four times with TBST for a total of 30 min. After which, the secondary antibodies conjugated with horseradish peroxidase at 1:5000 dilution for 1 h at room temperature and then washed four times with TBST. The blots were visualized with the Amersham ECL Plus Western blotting detection reagents according to the manufacturer's instructions. To assess the presence of comparable amounts of proteins in each lane, the membranes were stripped finally to detect the GAPDH.

3. Results and discussion

3.1. Chemistry

A well-developed method for synthesizing Ir(III) complex with a polypyridyl Ir(III) organometallic single-charged cation was used here [25–27], namely, the complex was obtained by the direction of two equivalents of ligand paip with cyclometalated Ir(III) dimers in CH_2Cl_2/CH_3OH (2:1, v/v) under reflux conditions. The product was precipitated out of the reacting mixture as hexafluorophosphate and purified by column chromatography. The authenticities of the complex can be confirmed by the data of ESI-MS and element analysis that are well in accord with the theoretical values. In the ^1H NMR spectra, the peak of 5.78 ppm is assigned to the hydrogen atoms in $-NH_2$.

3.2. Cell viability assay

The cell viability was evaluated by MTT assay. The results of cell viability were obtained after incubated with paip and complex **1** at different concentrations ranging from 0 to 100 μM against the selected cancer cell lines, and cisplatin was used as a positive control. The IC_{50} of paip and its complex are listed in Table 1. The cytotoxicity of ligand paip against SGC-7901, A549, HeLa, HepG-2 is higher than those of its corresponding complex. There were many cases that the

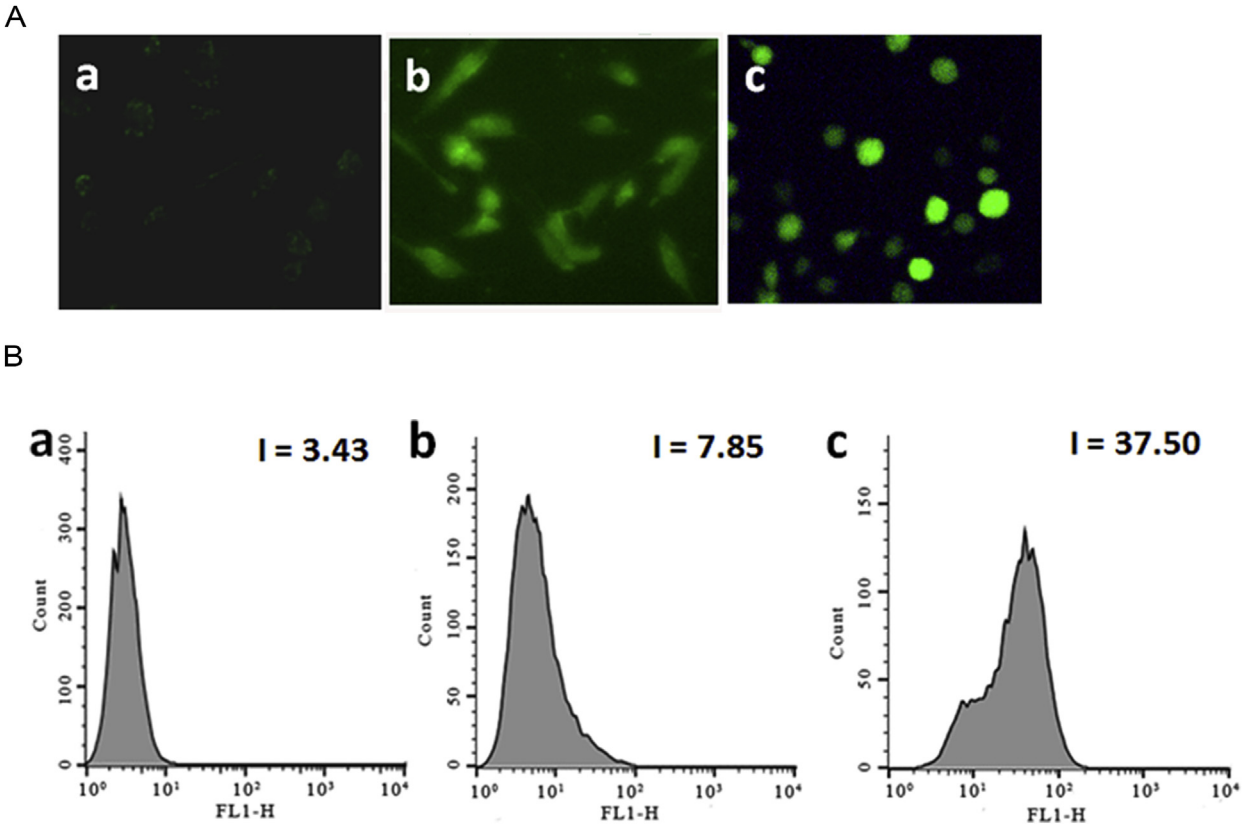

Fig. 3. A ROS generation in PC-12 cell (a) treated with Rosup (b, positive control) and 12.5 μM complex **1** (c). B DCF fluorescent intensity (I) was determined by flow cytometry after PC-12 cells (a) were treated with 6.25 (b) and 12.5 μM (c) of complex **1** for 24 h.

polypyridine such as APIP, HAPIP [26], OP (1,10-phenanthroline) [34], which was found to induce dramatically apoptotic cell death by an activation of p53. This we will conduct another study, and here we only focus on complex anticancer behaviors. As shown in Table 1, the complex has more striking anticancer activity than paip against SiHa, Bel-7402, PC-12. In particular, it is higher than cisplatin against PC-12 cells, this cell line was used to carry out the following cell biological experiments for the mechanism behind suppression of cell proliferation exert from complex.

3.3. Apoptosis induction in PC-12 by the complex

Apoptosis (known as a programmed cell death) is a fundamental and inherent biological event for maintaining the balance between cellular proliferation and death, evasion of apoptosis constitutes a characteristic feature of human cancers. Therapeutic strategies targeting inhibition of apoptotic resistance or induction of apoptosis represent a valid approach to develop effective anticancer drugs [35,36]. Here AO/EB and Annexin V-FITC/PI staining assays were respectively used for qualitative and quantitative investigating apoptosis. As shown in Fig. 1A, PC-12 cell (a) incubated in the absence of complex **1** was stained with uniform green fluorescence and no apoptotic features were observed. However, obvious morphological changes and green apoptotic cells (b) with features of blebbing, nuclear shrinkage and chromatin condensation were observed after the cells were treated with 6.25 μM (b) of complex **1** for 24 h. The results suggest that the complex induced PC-12 cell apoptosis. To further quantitatively compare the effect of the

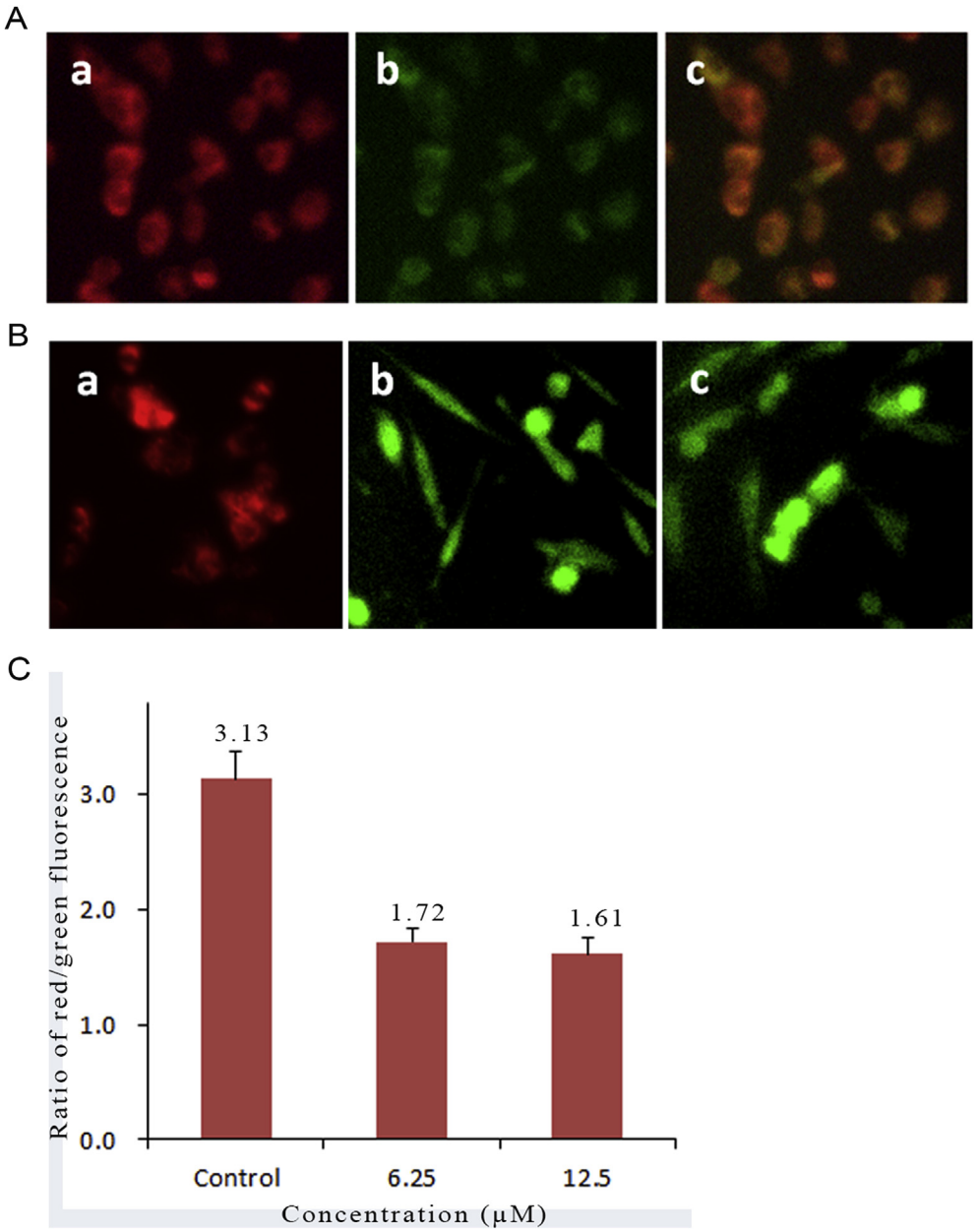

Fig. 4. A The localization of complex **1** in the mitochondria. Images of PC-12 cells treated with MTDRF (ThermoFisher, 80 nM) (a), 6.25 μM of **1** for 1 h (b) and the merge of a with b (c). The images were obtained by fluorescence microscope. B Assay of PC-12 cell mitochondrial membrane potential with JC-1 as fluorescent probe. PC-12 cells (*a*) exposure to cccp (*b*, positive control) and 6.25 μM (*c*) of **1** for 24 h. C The ratio of red/green fluorescent intensity was determined by flow cytometry after PC-12 line was treated with 6.25 and 12.5 μM of **1** for 24 h. (For interpretation of the references to colour in this figure legend, the reader is referred to the web version of this article.)

complex concentration on the apoptosis, the percentage in the apoptotic cells was determined using double staining of Annexin V and PI by flow cytometry. As shown in Fig. 1B, in the control (a), the percentages of apoptotic and necrotic cells are 0.41 and 8.08%. Comparing to the control, the percentages of apoptotic and necrotic cells treated with 6.25 (b) and 12.50 μM (c) of complex **1** are 0.95 and 7.95%, 2.22 and 12.84%, respectively. The results suggest that complex **1** induces apoptosis in PC-12 cell in dose-dependent manner.

3.4. Cellular uptake assay

It is well documented that iridium complexes show quick and efficient cellular internalization, their total cellular uptake reaches equilibrium just in half an hour [37]. Although, cylometalated Ir(III) complexes were proved to localize mainly in mitochondria; the ratio of $M_{mitochondria}/M_{cell}$ is about 80%, and nuclear absorption is below 10% [19,20,38], but the penetrating nucleus and binding to nuclear DNA may provide an important contribution to the mechanism of cytotoxicity [19]. To explore whether the present complex can enter into the cytoplasm and accumulate in the cell nuclei, the imaging experiment for PC-12 cells, which were treated with complex **1** (3.13 μM) or stained with nucleus-specific dye DAPI (4′,6-diamidino-2-phenylindole), were carried out with a fluorescent microscope, based on the color difference of fluorescence emitted between iridium complex and DAPI. As shown in Fig. 2, DAPI staining nucleus emits blue luminescence excited at 340 nm, and complex **1** emits green fluorescence with an excitation wavelength at 350 nm. The merged picture was obtained from the DAPI and complex **1** emission. Seen from the images, a plenty of green fluorescent spots in the cells can be found. The results show that the complex can transport across both the membrane and the envelope of subcellular organelle to accumulate in the cell nuclei.

3.5. ROS level and mitochondrial membrane potential (MMP) assay

The intracellular ROS is an important signaling molecule and can facilitate opening of the permeability transition pore complex and thus shifting the MMP [39]. H_2DFC-DA (non-fluorescent itself) is a cell permeable dye and can be used to evaluate the intracellular ROS levels, because it can be ultimately converted to a strongly emitting green fluorescent matter, *i.e.* dichlorofluorescein (DCF), by the intracellular ROS [40]. As shown in Fig. 3A, in the control (a), no obvious green spots were observed. After PC-12 cells were treated with Rosup (b, positive control) and 6.25 μM of complex **1** (c) for 24 h, a number of bright green spots were observed. The ROS level was further evaluated by detecting the DCF fluorescence intensity with flow cytometry. In the control (Fig. 3B (a)), the DCF fluorescence intensity is 3.43, after the treatment of PC-12 cells with 6.25 (b) and 12.5 μM (c) complex **1**, the DCF fluorescence intensity increases to 7.85 and 37.50 times than the control, respectively. These data suggest that complex **1** can increase the ROS levels with a concentration-dependent manner.

As power houses of cells, mitochondria play a vital role in core cellular metabolism in physiological and pathological scenarios, and their functions can be assessed by monitoring the changes in MMP [41]. A decrease in the MMP may be linked to the dysfunction of mitochondria and ultimately the apoptosis of the cells [42]. The polypyridyl cyclometalated iridium(III) complexes with various modified groups, such as aldehyde [18], chloromethyl [20], morpholine [38], ester [43], phenolic hydroxy [44] et al., have been proven to be potential mitochondria-targeting anticancer agents. In order to explore whether the apoptosis induction of complex **1** is through a mitochondria pathway, the experiments of mitochondria location and mitochondrial membrane potential detection were carried out. MitoTracker® Deep Red FM (MTDRF) is a mitochondrion-selective probe and is well-retained in the cell even during the process of fixation of permeabilization [45]. It is well suitable for labeling experiments at the present work because its red fluorescence is well resolved from the green fluorescence of the complex **1**. As shown in Fig. 4A, the mitochondria were stained in red with MTDRF (a), and the PC-12 cells treated with complex **1** (6.25 μM) emits green fluorescence (b). The merge (c) of the red and the green indicates that the complex can penetrate cell membrane and cumulate in the mitochondria. It is worth mentioning that all the biscylometalated Ir(III) complexes with a style of $[Ir(C,N)_2(N,N,N)]^+$ show the prefer accumulation in and targeting at mitochondria, the detailed action mechanism remains to be studied. The mitochondrion selectivity of this liposoluble cation with one charge may be partially resulting from cation-π interactions between the cation and circular DNA molecules in mitochondrion, being similar to the binding between Ach (acetylcholine) and cyclophane [46], this is just our speculation and needs more efforts to be confirmed in our future researches.

JC-1 is a liquid crystal-forming cationic dye and a reliable probe for analyzing MMP changes occurring very early in apoptosis [47,48]. Upon excitation at 490 nm, the JC-1 in cytoplasm or in mitochondrion at low membrane potential assumes monomer and displays a fluorescence emission centered at 537 nm (green), whereas it emits an intense fluorescence at 579 nm (red) when it aggregates in mitochondrion at high MMP [49]. The images of PC-12 cells (a) with cccp (b, carbonylcyanide-m-chlorophenylhydrazone, positive control) and 6.25 μM (c) of complex **1** were shown in Fig. 4B. In the control, JC-1 emits red fluorescence, and after the treatment with cccp and the complex, the JC-1 in treated cells emits green fluorescence. The changes from the red to green indicate that the complex can induce a decrease in the mitochondrial membrane potential. In order to quantitatively investigate the relationship between the effect on the changes of MMP and the concentration of complex **1** used, the ratios of red/green fluorescent intensity were determined by flow cytometry. In the control (Fig. 4C), the ratio of red/green fluorescence is 3.13, and when PC-12 cells were exposed to 6.25 and 12.50 μM of complex **1**, the ratios decrease to 1.72 and 1.61, respectively. This result confirms that the complex can induce a decrease in the MMP in a concentration-dependent manner.

3.6. Effect of the complex on cell cycle distribution and matrigel invasion

The effect of complexes **1** on cell cycle of PC-12 cells was studied

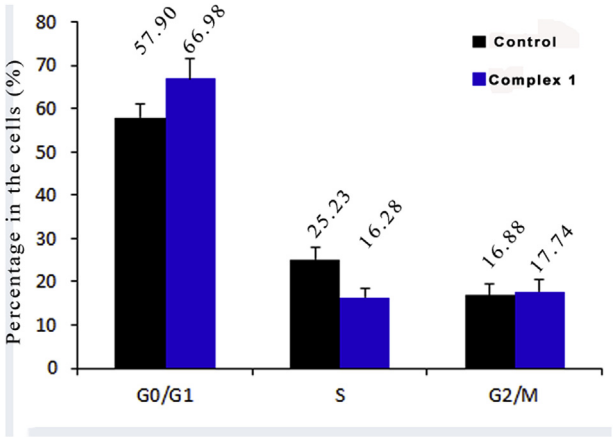

Fig. 5. The cell cycle arrest in PC-12 (black) induced by 12.5 μM of complex **1** (blue) for 24 h. (For interpretation of the references to colour in this figure legend, the reader is referred to the web version of this article.)

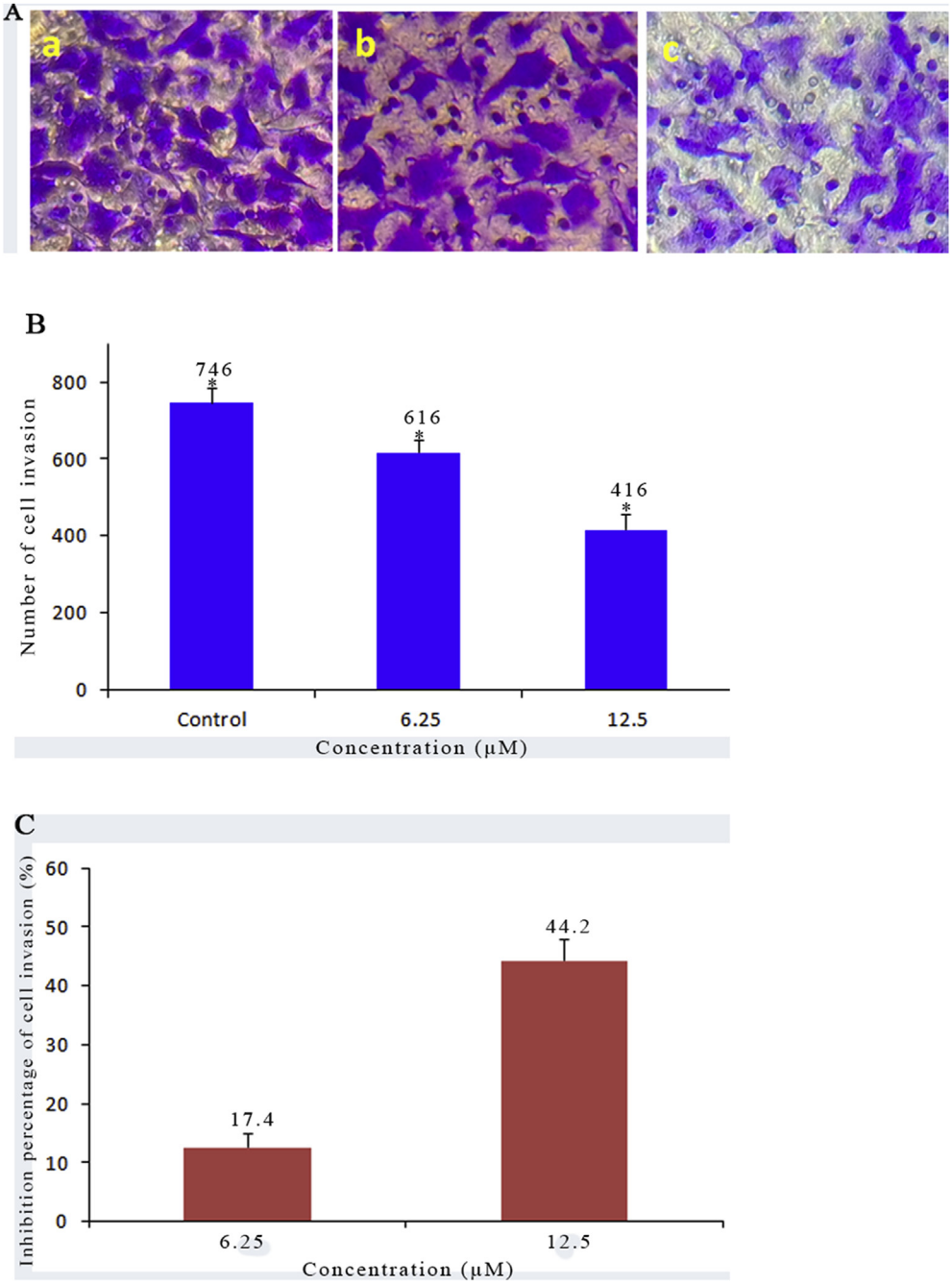

Fig. 6. A Microscope images of invading PC-12 cells (*a*) that have migrated through the Matrigel induced by 6.25 (*b*) and 12.50 μM (*c*) of complex **1** for 24 h. B Cell invasion assay result of **1** against PC-12 cell. $^{*}P < 0.05$ represents significant differences compared with control. C The percentage of inhibiting cell invasion at 6.25 and 12.5 μM of **1**.

by estimating the relative number of cells in the different phases of the mitotic cycle *via* fluorescence-activated (*i.e.* propidium iodide stained) cell sorting. As shown in Fig. 5, in the control (a), the percentage in the cells at G0/G1 is 57.90%. Following treatment with 12.5 μM of complexes **1**, the percentage in the cells at G0/G1 is 66.98%. An obvious increase of 9.08% at G0/G1 phase compared with the control was found, accompanied by a reduction of 8.95% at S phase. This result indicates that the complex inhibits PC-12 cell growth at G0/G1 phase.

Meanwhile, it is well commonly accepted that the tumor invasion of basement membranes is one of the crucial steps in the complex multistep event resulting to the successful formation of a metastasis [50]. The transwell invasion assay for PC-12 cells was studied by Matrigel invasion assay. As shown in Fig. 6, the number of the invasion cells decrease upon being exposed to complex **1**, and the percentages of cell invasion inhibiting by complex **1 at** 6.25 and 12.5 μM are calculated to be 17.4% and 44.2%, respectively. These results demonstrate that the complex can effectively inhibit PC-12 cell invasion and shows a concentration-dependent manner.

3.7. The expression of caspases and Bcl-2 family proteins

Caspase-3 and -7 are executioners of apoptosis as processing of their substrates lead to morphological changes associated with apoptosis, including DNA degradation, chromatin condensation, and membrane blebbing [51].

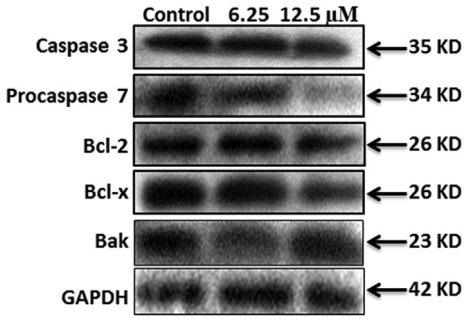

Fig. 7. Western blot analysis of caspase 3, caspase 7, Bcl-2, Bcl-x, Bak in PC-12 cells treated with different concentration of complex **1** for 24 h. GAPHD was used as internal control.

The activation of caspase 3 and procaspase 7 was assayed by western blot. As shown in Fig. 7, after the treatment of PC-12 cells with 6.25 and 12.50 μM of complexes **1** for 24 h, the expression of caspase 3 was up-regulated, whereas the expression level of procaspase 7 was down-regulated. Bcl-2 family proteins include anti-apoptotic such as Bcl-2 and Bcl-x and proapoptotic proteins such as Bak and Bid. Treatment of PC-12 cells with the complex led to a decrease in the expression of Bcl-2 and Bcl-x, and induced an increase in the expression of Bak and Bid. The results suggest that the complex can regulate the expression levels of Bcl-2 family proteins.

4. Conclusions

A polypyridyl Ir(III) organometallic complex, $[Ir(ppy)_2(paip)]PF_6$ **1**, was synthesized and characterized. The complex shows high cytotoxic activity in vitro toward PC-12 cells. Complex **1** can cause apoptosis, increase the ROS levels and induce a decrease in the mitochondrial membrane potential. And the complex inhibits the cell growth in PC-12 cells at G0/G1 phase. Cell invasion assay showed that the complex can effectively inhibit the cell invasion and activate caspase 3 and procaspase 7, down-regulate the expression of Bcl-2 and Bcl-x, up-regulate the expression levels of Bak. In summary, the complex induces apoptosis in PC-12 cell through a ROS-mediated mitochondrial dysfunction pathway. This work is helpful for developing non-platinum anticancer drugs.

Acknowledgments

This work was supported by the Natural Science Foundation of Guangdong Province (Nos 2016A030313728, 2014A030307015), Featured Innovation in Colleges and Universities of Guangdong Province Project (2014KTSCX169) and Shaoguan University (Sycxcy2017-129).

Appendix A. Supplementary data

Supplementary data related to this article can be found at http://dx.doi.org/10.1016/j.jorganchem.2017.07.004

References

[1] H.K. Liu, P.J. Sadler, Metal complexes as DNA intercalators, Accounts Chem. Res. 44 (2011) 349–359.
[2] U. Ndagi, N. Mhlongo, M. Esoliman, Metal complexes in cancer therapy–an update from drug design perspective, Drug Des. Dev. Ther. 11 (2017) 599–616.
[3] D. Chen, V. Milacic, M. Frezza, Q.P. Dou, Metal complexes, their cellular Targets and potential for cancer therapy, Curr. Pharm. Des. 15 (2009) 777–791.
[4] P.C.A. Bruijnincx, P.J. Sadler, New trends for metal complexes with anticancer activity, Curr. Opin. Chem. Biol. 12 (2008) 197–206.
[5] P. Zhang, P.J. Sadler, Advances in the design of organometallic anticancer complexes, J. Organomet. Chem. 839 (2017) 5–14.
[6] J. Skiba, T. Bernás, D. Trzybiński, K. Wózniak, G. Ferraro, D. Marasco, A. Merlino, M.Z. Shafikov, R. Czerwieniec, K. Kowalski, Mitochondria targeting with luminescent rhenium(I) complexes, Molecules 809 (2017) 1–17.
[7] K. Kowalski, Ferrocenyl-nucleobase complexes: synthesis, chemistry and applications, Coord. Chem. Rev. 317 (2016) 132–156.
[8] G. Jaouen, A. Vessières, S. Top, Ferrocifen type anti cancer drugs, Chem. Soc. Rev. 44 (2015) 8802–8817.
[9] J. Liu, W. Zheng, S. Shi, C. Tan, J. Chen, K. Zheng, L. Ji, Synthesis, antitumor activity and structure–activity relationships of a series of Ru(II) complexes, J. Inorg. Biochem. 102 (2008) 193–202.
[10] J.Q. Wang, P.Y. Zhang, L.N. Ji, H. Chao, A ruthenium(II) complex inhibits tumor growth in vivo with fewer side-effects compared with cisplatin, J. Inorg. Biochem. 146 (2015) 89–96.
[11] M.R. Gill, J.A. Thomas, Ruthenium(II) polypyridyl complexes and DNA–from structural probes to cellular imaging and therapeutics, Chem. Soc. Rev. 41 (2012) 3179–3192.
[12] C.S. Devi, P. Nagababu, V.V. Reddy, V. Sateesh, A. Srishailam, S. Satyanarayana, Synthesis, characterisation, interaction with DNA, cytotoxicity, and apoptotic studies of ruthenium(II) polypyridyl complexes, Aust. J. Chem. 67 (2014) 225–233.
[13] M.J. Bloemink, J. Reedijk, Cisplatin and derived anticancer drugs: mechanism and current status of DNA binding, Met. ions Boil. Syst. 32 (1996) 641–685.
[14] P. Umapathy, The chemical and biochemical consequences of the binding of the antitumour drug cisplatin and other platinum group metal complexes to DNA, Coord. Chem. Rev. 95 (1989) 129–181.
[15] L. Helm, A.E. Merbach, Water exchange on metal ions: experiments and simulations, Coord. Chem. Rev. 187 (1999) 151–181.
[16] K. Xiong, Y. Chen, C. Ouyang, R.L. Guan, L.N. Ji, H. Chao, Cyclometalated iridium(III) complexes as mitochondria-targed anticancer agents, Biochimie 125 (2016) 186–194.
[17] S.K. Leung, H.W. Liu, K. Kam-Wing Lo, Functionalization of Luminescent Cyclometalated Iridium(III) Polypyridine Complexes with a Fluorous Moiety: Photophysics, Protein-binding, Bioconjugation, and Cellular Uptake Properties vol. 47, 2011, pp. 10548–10550.
[18] P.K. Lee, H.W. Liu, S.M. Yiu, M.W. Louie, K. Kam-Wing Lo, Luminescent cyclometallated iridium(III) bis(quinolylbenzaldehyde) diimine complexes—synthesis, photophysics, electrochemistry, protein cross-linking properties, cytotoxicity and cellular uptake, J. Chem. Soc. Dalton Trans. 40 (2011) 2180–2189.
[19] Z. Liu, A. Habtemariam, A.M. Pizarro, S.A. Fletcher, A. Kisova, O. Vrana, L. Salassa, P.C.A. Bruijnincx, G.J. Clarkson, V. Brabec, P.J. Sadler, Organometallic half-sandwich iridium anticancer complexes, J. Med. Chem. 54 (2011) 3011–3026.
[20] J.J. Cao, C.P. Tan, M.H. Chen, N. Wu, D.Y. Yao, X.G. Liu, L.N. Ji, Z.W. Mao, Targeting cancer cell metabolism with mitochondria-immobilized phosphorescent cyclometalated iridium(III) complexes, Chem. Sci. 8 (2017) 631–640.
[21] E. Sauvageot, P. Lafite, E. Duverger, R. Marion, M. Hamel, S. Gaillard, J.L. Renaud, R. Daniellou, Iridium complexes inhibit tumor necrosis factor-a by utilizing light and mixed ligands, J. Organomet. Chem. 808 (2016) 122–127.
[22] H. Huang, P. Zhang, B. Yu, Y. Chen, J. Wang, L. Ji, H. Chao, Targeting nucleus DNA with a cyclometalated dipyridophenazineruthenium(II) complex, J. Med. Chem. 57 (2014) 8971–8983.
[23] S. Schäfer, I. Ott, R. Gust, W.S. Sheldrick, Influence of the polypyridyl (pp) ligand size on the DNA binding properties, cytotoxicity and cellular uptake of organoruthenium(II) complexes of the type $[(\eta^6\text{-}C_6Me_6)Ru(L)(pp)]^{n+}$, Eur. J. Inorg. Chem. (2007) 3034–3046.
[24] H. Yu, J. Liu, Z. Hao, J. He, M. Sun, S. Hu, L. Yu, H. Chao, Synthesis, characterization and biological evaluation of ruthenium(II) complexes Ru(dtzp)(dppz)Cl]$^+$ and $[Ru(dtzp)(dppz)CH_3CN]^{2+}$ for photodynamic therapy, Dyes Pigments 136 (2017) 416–426.
[25] K. Qiu, Y. Liu, H. Huang, C. Liu, H. Zhu, Y. Chen, L. Ji, H. Chao, Biscylometalated iridium(iii) complexes target mitochondria or lysosomes by regulating the lipophilicity of the main ligands, Dalton Trans. 45 (2016) 16144–16147.
[26] M. Nonoyama, Benzo[h]quinolin-10-yl-N iridium(III) complexes, Bull. Chem. Soc. Jpn. 47 (1974), 768–768.
[27] S. Sprouse, K.A. King, P.J. Spellane, R.J. Watts, Photophysical effects of metal-carbon σ bonds in ortho-metalated complexes of Ir(III) and Rh(III), J. Am. Chem. Soc. 106 (1984) 6647–6653.
[28] C.H. Zeng, H.L. Huang, L.X. He, F.H. Wu, Synthesis, DNA-binding, photocleavage, cytotoxicity and antioxidant activity of ruthenium (II) polypyridyl complexes, Eur. J. Med. Chem. 45 (2010) 564–571.
[29] Y.J. Liu, Z.H. Liang, Z.Z. Li, J.H. Yao, H.L. Huang, Cellular uptake, cytotoxicity, apoptosis, antioxidant activity and DNA binding of polypyridyl ruthenium(II) complexes, J. Organomet. Chem. 696 (2011) 2728–2735.
[30] H.L. Huang, Y.J. Liu, C.H. Zeng, L.X. He, F.H. Wu, In vitro cytotoxicity, apoptosis, DNA-binding, and antioxidant activity studies of ruthenium (II) complexes, DNA Cell Biol. 29 (2010) 261–270.
[31] T. Mosmann, Utilization of purified human monocytes in the agarose droplet assay for measuring migration inhibitory factors, J. Immunol. Methods 65 (1983) 55–63.
[32] D.L. Spector, R.D. Goldman, L.A. Leinwand, In Cells: a Laboratory Manual vol. 1, Cold Spring Harbor Laboratory Press, New York, 1998 (Chapter 15).
[33] K.K. Lo, T.K. Lee, J.S. Lau, W.L. Poon, S.H. Cheng, Luminescent biological probes derived from ruthenium(II) estradiol polypyridine complexes, Inorg. Chem. 47

(2008) 200–208.
[34] Y. Sun, J. Bian, Y. Wang, C. Jacobs, Activation of p53 transcriptional activity by 1,10-phenanthroline, a metal chelator and redox sensitive compound, Oncogene 14 (1997) 385–393.
[35] S. Fulda, Targeting apoptosis for anticancer therapy, Semin. Cancer Biol. 31 (2015) 84–88.
[36] G. Pistritto, D. Trisciuoglio, C. Ceci, A. Garufi, G. D'Orazi, Apoptosis as anticancer mechanism: function and dysfunction of its modulators and targeted therapeutic strategies, Aging 8 (2016) 603–619.
[37] J. Liu, C. Jin, B. Yuan, X. Liu, Y. Chen, L. Jia, H. Chao, Selectively lighting up two-photon photodynamic activity in mitochondria with AIE-active iridium(III) complexes, Chem. Comm. 12 (2017) 2052–2055.
[38] K. Qiu, H. Huang, B. Liu, Y. Liu, P. Zhang, Y. Chen, L. Ji, H. Chao, Mitochondria-specific imaging and tracking in living cells with two-photon phosphorescent iridium(III) complexes, J. Mater. Chem. B 32 (2015) 6690–6697.
[39] B. Zhang, D. Wang, F. Guo, C. Xuan, Mitochondrial membrane potential and reactive oxygen species in cancer stem cells, Fam. Cancer 14 (2015) 19–23.
[40] L.R. Silveira, L. Pereira-Da-Silva, C. Juel, Y. Hellsten, Formation of hydrogen peroxide and nitric oxide in rat skeletal muscle cells during contractions, Free Radic. Biol. Med. 35 (2003) 455–464.
[41] S. Sakamuru, M.S. Attene-Ramos, M. Xia, Mitochondrial membrane potential assay, High-Throughput Screen. (HTS) Assays Toxicol. 1473 (2016) 17–22.
[42] J.J. Lemasters, T. Qian, L. He, J.S. Kim, S.P. Elmore, W.E. Cascio, D.A. Brenner, Role of mitochondrial inner membrane permeabilization in necrotic cell death, apoptosis, and autophagy, Antioxid. Redox. Signal 4 (2002) 769–781.
[43] F.X. Wang, M.H. Chen, X.Y. Hu, R.R. Ye, C.P. Tan, L.N. Ji, Z.W. Mao, Ester-modified cyclometalated iridium(III) complexes as mitochondria-targeting anticancer agents, Sci. Rep. 6 (2016) 38954–38968.
[44] J. Wang, X. Hou, C. Jin, H. Chao, A cyclometalated iridium(III) complex serves as a phosphorescent probe for specific mitochondrial imaging in living cells, Chin. J. Chem. 34 (2016) 583–588.
[45] Invitrogen™, Molecular Probes® Invitrogen Detection Technologies, MitoTracker® Mitochondrion-selective Probes, 2008, pp. 1–5. MP07510.
[46] D.A. Dougherty, Cation-π interactions in chemistry and biology: a new view of benzene, phe, tyr, and trp, Science 271 (1996) 163–168.
[47] A. Cossarizza, M. Baccarani-Contri, G. Kalashnikova, C. Fraceschi, A new method for cytofluorimetric analysis of mitochondrial membrane potential using the J-aggregate forming lipophilic cation 5,5',6,6'-tetrachloro-1,1',3,3'-tettraethylbenzimidazol-carbocyanine iodine (JC-1), Biochem. Biophys. Res. Commun. 197 (1993) 40–45.
[48] S.T. Smiley, M. Reers, C. Mattola-Hartshorn, M. Lin, A. Chen, T.W. Smith, G.D.J. Steele, L.B. Chen, Intracellular heterogeneity in mitochondrial membrane potentials revealed by a J-aggregate forming lipophilic cation JC-1, Proc. Natl. Acad. Sci. U. S. A. 88 (1991) 3671–3675.
[49] O. Legrand, J.Y. Perrot, G. Simonin, M. Baudard, J.P. Marie, JC-1: a very sensitive fluorescent probe to test Pgp activity in adult acute myeloid leukemia, Blood 97 (2001) 502–508.
[50] M. Debbie, S.A. Brooks, In vitro invasion assay using Matrigel®, Metastasis Res. Protoc. 58, 61–70.
[51] N.A. Thornberry, Y. Lazebnik, Caspases: enemies within, Science 281 (1998) 1312–1316.